

## Cellulose nanofibers production using a set of recombinant enzymes

Bruno R. Rossi<sup>a</sup>, Vanessa O.A. Pellegrini<sup>a</sup>, Anelyse A. Cortez<sup>a</sup>, Emanoele M.S. Chiromito<sup>b</sup>, Antonio J.F. Carvalho<sup>b</sup>, Lidiane O. Pinto<sup>c</sup>, Camila A. Rezende<sup>c</sup>, Valmor R. Mastelaro<sup>a</sup>, Igor Polikarpov<sup>a,\*</sup>

<sup>a</sup> São Carlos Institute of Physics, University of São Paulo, Av. Trabalhador São-carlense, 400, São Carlos, SP, 13566-590, Brazil

<sup>b</sup> Materials Science and Engineering Department, São Carlos School of Engineering, University of São Paulo, Av. João Dagnone, 1100, São Carlos, SP, 13563-120, Brazil

<sup>c</sup> Institute of Chemistry, University of Campinas, P.O. Box 6154, 13083-970, Campinas, SP, Brazil

### ARTICLE INFO

#### Keywords:

Cellulose nanofiber  
Sugarcane bagasse  
Enzyme  
Sonication  
CNF

### ABSTRACT

Cellulose nanofibers (CNF) are renewable and biodegradable nanomaterials with attractive barrier, mechanical and surface properties. In this work, three different recombinant enzymes: an endoglucanase, a xylanase and a lytic polysaccharide monoxygenase, were combined to enhance cellulose fibrillation and to produce CNF from sugarcane bagasse (SCB). Prior to the enzymatic catalysis, SCB was chemically pretreated by sodium chlorite and KOH, while defibrillation was accomplished via sonication. We obtained much longer ( $\mu\text{m}$  scale length) and more thermostable (resisting up to 260 °C) CNFs as compared to the CNFs prepared by TEMPO-mediated oxidation. Our results showed that a cooperative action of the set of hydrolytic and oxidative enzymes can be used as a “green” treatment prior to the sonication step to produce nanofibrillated cellulose with advanced properties.

### 1. Introduction

Nanocelluloses are promising new eco-friendly products obtained from lignocellulosic biomass with at least one dimension in the nanoscale (Klemm et al., 2018). These nanomaterials show exceptional functionalities such as excellent mechanical properties, large surface area, hydrophilicity and the omnipresence of interacting surface hydroxyl groups that provides a platform for significant modification of surface properties (De France, Hoare, & Cranston, 2017; Dufresne, 2019). As a result, these emerging sustainable nanomaterials exhibit diverse applications in different areas, such as biomedicine, food packaging, electronics and cosmetics, and attract increasing investment (Lin & Dufresne, 2014; Phanthong et al., 2018).

The three main types of nanocelluloses are cellulose nanofibers (CNF), cellulose nanocrystals (CNC), and bacterial cellulose (BC), which show variations in their dimensions, morphology and preparation methods (Lin & Dufresne, 2014; Liu, Kerr, & Kong, 2019; Wang, Tavakoli, & Tang, 2019; Yue et al., 2019). For CNC and CNF, morphology and dimensions depend on the cellulose source and on the production protocol (Blanco et al., 2018; Habibi, Lucia, & Rojas, 2010; Moon, Martini, Nairn, Simonsen, & Youngblood, 2011). Cellulose nanofibers, also known as nanofibrillated cellulose, have an average diameter of approximately 5–60 nm and can have several micrometers in length,

forming long and flexible nanofibers that alternate crystalline and amorphous domains (Blanco et al., 2018; Klemm et al., 2011). Typical sources for CNF production are wood, seed fibers, bast fibers and grasses (bagasse, bamboo, etc.), among others (Klemm et al., 2011).

In the present work, sugarcane bagasse was chosen to produce CNF, due to its abundance and relatively low recalcitrance (Pinto, Bernardes, & Rezende, 2019). Brazil is the world's largest sugarcane producer with approximately 657 million tons of the sugarcane plant grown and collected per year, which leads to a generation of about 160 million tons of sugarcane bagasse (SCB) annually (Companhia Nacional do Abastecimento (CONAB), 2020). Although a major fraction of the SCB nowadays is used for energy production and, increasingly, for second generation ethanol, it is estimated that about 17 % (approximately 27 million tons) of the remaining bagasse is not productively utilized, becoming an agricultural waste (Ministério de Minas e Energia (MME), 2019). Thus, SCB can be used as a low-cost industrial feedstock for the production of high added value materials such as nanocellulose (Mandal & Chakrabarty, 2011; Oliveira, Bras, Pimenta, Curvelo, & Belgacem, 2016).

For CNF production, cellulose must be first isolated from the natural sources (Mokhena & John, 2020). Accordingly, an initial pretreatment to remove lignin and hemicellulose from SCB is necessary, followed by one or more bleaching steps (Klemm et al., 2018; Nechyporchuk,

\* Corresponding author.

E-mail address: [ipolikarpov@ifsc.usp.br](mailto:ipolikarpov@ifsc.usp.br) (I. Polikarpov).

<https://doi.org/10.1016/j.carbpol.2020.117510>

Received 30 August 2020; Received in revised form 20 November 2020; Accepted 9 December 2020

Available online 15 December 2020

0144-8617/© 2020 Elsevier Ltd. All rights reserved.

Belgacem, & Bras, 2016). After obtaining a cellulose-enriched material, homogenizers, micro-fluidizers and grinders are usually employed to promote cellulose mechanical defibrillation (Nechporchuk et al., 2016; Rol, Belgacem, Gandini, & Bras, 2019). Despite being widely applied, these promising approaches have some limitations and drawbacks (Nechporchuk et al., 2016; Rol et al., 2019). A main drawback of the mechanical processes is a high energy consumption. Furthermore, mechanical treatments typically result in low solid density aqueous dispersions of CNFs (below 5%), which can incur in high transportation costs and storing challenges.

Various chemical treatments can be applied to the isolated cellulose to reduce the energy demand and to facilitate the mechanical action, including cationization, carboxymethylation and TEMPO-mediated oxidation (Errokh, Magnin, Putaux, & Boufi, 2018; Tejado, Alam, Antal, Yang, & van de Ven, 2012). Although being increasingly efficient, there are still major environmental issues related to the utilization of these chemicals for CNF production, particularly for TEMPO-mediated oxidation (Hu, Tian, Rennecker, & Saddler, 2018). A new approach used to ease cellulose fibrillation via mechanical methods is an enzymatic treatment (Rol et al., 2019). This approach has received increasing attention due to high substrate specificity of enzymes that leads to reduced energy consumption for fibrillation and its environmentally friendly aspects (Farinas, Marconcini, & Mattoso, 2018; Koskela et al., 2019).

Several studies have been carried out to investigate the use of endoglucanases to enhance cellulose fibrillation for CNF production (Hu et al., 2018; Martelli-Tosi et al., 2018; Ribeiro, Pohlmann, Calado, Bojorge, & Pereira, 2019). These enzymes predominantly cleave glycosidic linkages within cellulose amorphous regions, producing new cellulose chain ends and releasing short chain oligosaccharides, thus facilitating refining and fibrillation (Sonoda et al., 2019). Auxiliary enzymes such as xylanases and lytic polysaccharide monooxygenases (LPMO) were recently proposed to promote cellulose fibrillation via enzymatic hydrolysis and oxidative mechanisms (Hu et al., 2018). Xylanases do not directly hydrolyze cellulose, but facilitate the access to the cellulose fibers by removing adsorbed xylan, whereas LPMOs selectively modify the carbohydrate network by oxidation, thus inserting negative charges at the surface of cellulose and facilitating fibrillation (Hu, Arantes, Pribowo, Gourlay, & Saddler, 2014).

Xylanases have been shown to hydrolyze the glycosidic linkages of hemicelluloses, peeling off xylan chains from the cellulose surface (Evangelista et al., 2019; Hu, Arantes, & Saddler, 2011). In addition, application of xylanases provides means to transform xylans into renewable fuels and value-added products (Sepulchro et al., 2020). Furthermore, these enzymes act synergistically with cellulases to enhance fiber characteristics by increasing fiber swelling and porosity (Hu et al., 2018). LPMOs oxidatively cleave glycosidic linkages at either the C1 or C4 position, resulting in production of aldonic acids or gem-diols, respectively (Westereng et al., 2016). The enzymes introduce ionizable carboxyl groups at the fiber surface, thus disrupting the highly organized cellulose structure and acting as cellulose chain breakers, which renders the substrate more susceptible to be hydrolyzed by conventional cellulases (Kadowaki et al., 2018; Simmons et al., 2017). Similar to TEMPO-oxidation, the resulting carboxyl groups inserted by LPMO on fiber surfaces have been shown to facilitate cellulose fibrillation due to the increased surface charge and reduced fiber aggregation of the produced CNFs (Hu et al., 2018).

Several studies reported the utilization of these enzymes separately (Koskela et al., 2019; Nie et al., 2018; Zhang, Zhang, Yan, Zhang, & Nie, 2018; Zhou, St. John, & Zhu, 2019) or in combination (Bian et al., 2019; Hu et al., 2018) for CNF production, but very few of them focused on sugarcane bagasse as a lignocellulosic source (de Campos et al., 2013; Saelee, Yingkamhaeng, Nimchua, & Sukyai, 2016). Saelee et al. (2016) used only xylanase treatment prior to mechanical disintegration to produce CNF from SCB. On the other hand, de Campos et al. (2013) used endoglucanase and a mix of hemicellulases and pectinases prior to

sonication to obtain cellulose nanofibers from sugarcane bagasse and curauá fibers. They showed that CNF produced from SCB required lower enzyme loadings than CNF from curauá, thus indicating that it is easier to produce CNF from the former fibers (de Campos et al., 2013). In addition, there is only one report so far in which a set of endoglucanase, xylanase and LPMO was used in combination to produce CNF (Hu et al., 2018), but SCB was not used as a raw material. Hu et al. (2018) showed that treatment of a fully bleached hardwood Kraft pulp with these three different enzymes in combination enabled nanofibrillation through mechanical sonication without sacrificing CNF thermostability. Therefore, combining enzymatic treatment with mechanical disintegration opens up possibilities for the production of CNFs with advanced features, besides representing an environmentally friendly way to reduce energy demands in subsequent mechanical process.

In the present work, we assessed a potential of a set of three different recombinant enzymes, GH7 endoglucanase from *Trichoderma harzianum* (ThCel7B), GH10 xylanase from *Thermobacillus composti* (TcXyn10A), and AA9 LPMO from *Thermothelomyces thermophilus* (TLPMO9H), capable of acting in combination to enhance cellulose fibrillation for CNF production from SCB. GH7 family endoglucanases are known to act on a number of different substrates apart from cellulose, including xylan, xyloglucan, beta-glucan and lichenan (Pellegrini et al., 2015; Vlasenko, Schülein, Cherry, & Xu, 2010). In fact, for several enzymes of this family, including *Trichoderma harzianum* enzyme used in current study, the enzymatic activity on hemicellulosic substrates is higher than their activities on non-decorated and highly recalcitrant crystalline cellulose (Vlasenko et al., 2010). Thus, together with the xylanase TcXyn10A used in our experiments, ThCel7B is expected to act on SCB arabinoxylans. Previous studies of GH7 cellulases from *T. harzianum* demonstrated that ThCel7B also efficiently hydrolyzed both filter paper and bacterial cellulose, introducing clear morphological changes in these substrates and displaying considerable synergy with an exoglucanase ThCel7A (Pellegrini, Bernardes, Rezende, & Polikarpov, 2018). Furthermore, ThCel7B type 1 CBM was shown to efficiently introduce morphological changes in the cellulosic substrates, leading to improved access of cellulases to the substrate and to an enhanced generation of insoluble reducing ends (Bernardes et al., 2019). Taken together, one would expect that ThCel7B endoglucanase would hydrolyze the xylan available in the samples and facilitate cellulose fibrillation by predominantly introducing hydrolytic cuts in the amorphous parts of the cellulose fibers, and also promote partial separation of the cellulose bundles by its type 1 CBM (Bernardes et al., 2019). Moreover, endoglucanases from GH7 family were shown to demonstrate a strong synergy with AA9 LPMOs (Keller et al., 2020). All these evidences allow us to conclude that a chosen mixture of the three recombinant enzymes, ThCel7B GH7 endoglucanase, TcXyn10A GH10 xylanase and TLPMO9H AA9 LPMO is expected to hydrolyze xylan fraction attached to cellulose and also erode amorphous regions of the cellulose preferentially, while inserting carboxyl groups at the cellulose surface as a result of LPMO activity.

In the work reported here, prior to the enzymatic catalysis, SCB was chemically pretreated by sodium chlorite and KOH solutions, following Grande, Trovatti, Pimenta, and Carvalho (2018), while defibrillation was finished through relatively mild sonication, as compared to more intense sonication regimes reported in previous works (de Campos et al., 2013; Chen et al., 2011). We assessed the overall fiber morphology, crystallinity, oxidized group content and thermostability after enzymatic treatment and compared enzymatically-produced CNFs with those obtained by TEMPO-oxidation. Our results demonstrated that the CNFs produced from SCB by a "green" biocatalytic route using enzymes resulted in significantly longer and more thermostable CNFs as compared to the fibers obtained via TEMPO-oxidation.

## 2. Material and methods

### 2.1. The enzymes

*ThCel7B*, *TcXyn10A* and *TtLPMO9H* were heterologously produced. *ThCel7B* was expressed in *Aspergillus niger*, as previously described (Pellegrini et al., 2015). Briefly, a minimal medium supplied with maltose was used as a carbon source and a cultivation under static conditions was carried out at 30 °C for 6 days. The first step of purification started with overnight precipitation by ammonium sulfate at 80 % saturation, followed by protein purification using hydrophobic chromatography with a Phenyl-Sepharose 6 Fast Flow column (GE Healthcare Biosciences, Little Chalfont, UK). The second purification step was accomplished by molecular exclusion chromatography, using a Superdex 75 16/60 column. *ThCel7B* has a specific activity of 16 U/mg and 12 U/mg towards rye arabinoxylan and beechwood glucuronoxylan, respectively (Pellegrini et al., 2015). The enzyme also has specific activity of approximately 0.4 U/mg on filter paper and 0.3 U/mg on Avicel (Pellegrini et al., 2015).

*TtLPMO9H* was expressed in *Aspergillus nidulans*, using inducing medium (minimal medium with 3% of HIGH maltose and pyridoxine 1 mg/L) at 37 °C for two days and under static conditions. The protein was purified following the same purification protocol as described above for *ThCel7B*. Before size exclusion chromatography, *TtLPMO9H* was saturated with copper, using a solution of copper sulphate with molar concentration 3 times higher in comparison to the protein molar concentration (Loose, Forsberg, Fraaije, Eijsink, & Vaaje-kolstad, 2014). The enzyme activity on cellulose was confirmed using high-performance liquid chromatography with pulsed amperometric detection (HPLC PAC).

*TcXyn10A* production followed the protocol described in Sepulchro et al. (2020). In short, heterologous expression was performed using 2xYT liquid medium, at 37 °C and 200 rpm in a shaker for 4 h until the cell density reached an OD<sub>600</sub> of 0.6. Then, the grown cells were induced with 0.5 mM isopropyl β-D-thiogalactopyranoside (IPTG) at 20 °C under continuous agitation at 200 rpm in a shaker overnight. The culture was centrifuged and the cell pellet was resuspended in a lysis buffer followed by three cycles of freezing and thawing in liquid nitrogen and more six cycles (30 s on and 30 s off) of sonication with ultrasonic probe at 40 % of amplitude. The lysate was clarified by centrifugation to remove cell debris and the supernatant was purified using a Ni-NTA Superflow column (Qiagen, Hilden, Germany). The protein was eluted with gradient of imidazole, and the protein was incubated with recombinant Tobacco Etch Virus (TEV) protease for 6xHis-thioredoxin tag removal from the target enzyme. A final size-exclusion chromatography step was performed in the Äkta Purifier 10 (GE Healthcare, Chicago, USA) system using a HiLoad 16/600 Superdex 75 pg column (GE Healthcare, Chicago, USA). *TcXyn10A* has a specific activity of 117 U/mg on rye arabinoxylan and 101 U/mg on beechwood glucuronoxylan (Sepulchro et al., 2020).

### 2.2. Sugarcane bagasse pretreatment

To obtain a cellulose-rich substrate for fibrillation, a two-step pretreatment using sodium chlorite and potassium hydroxide was performed, according to Grande et al. (2018). First, SCB was washed, dried and knife milled. Then, approximately 5 g of the milled sample was added to 0.4 L of a 1.3 % w/v NaClO<sub>2</sub> solution at pH 4. The sample was kept at 65 °C under magnetic stirring in a water bath for one hour, before filtering under vacuum. In the second alkaline step with KOH, the solid filtered sample was added to 0.6 L of a 2% w/v KOH solution and kept under magnetic stirring at 85 °C in a water bath for two hours, followed by another filtration in a vacuum system. Both the bleaching step with NaClO<sub>2</sub> and the delignification step with KOH were performed twice each, in an intercalated manner.

### 2.3. Chemical composition of lignocellulosic materials

The chemical composition of untreated and pretreated sugarcane bagasse was obtained according to a protocol established by Rocha et al. (1997) and validated by Gouveia, do Nascimento, Souto-Maior, and de M. Rocha (2009). Initially, the solid samples were knife milled, passed through a 20-mesh sieve and had their dry matter weight determined. Extractives (waxes, lipids and tannins) were removed from the untreated bagasse, using a 1:1 cyclohexane/ethanol solvent mixture (Park, Doherty, & Halley, 2008). After extraction, samples were dried and the content of extractives was determined.

Monosaccharide content of the samples obtained after acid hydrolysis were analyzed by high performance liquid chromatography (HPLC) using an Aminex column (HPX-87H, 300 × 7.8 mm, Bio-Rad, USA) in a Shimadzu LC-10AD chromatograph equipped with refractive index and UV-vis detector (Espírito Santo et al., 2018). The mobile phase was H<sub>2</sub>SO<sub>4</sub> (5.10<sup>-3</sup> mol/L) with the flow rate of 0.6 mL.min<sup>-1</sup> and this isocratic condition was maintained for 1 h at 65 °C.

### 2.4. Nanofibrillation by enzymatic pretreatment

Pretreated SCB was enzymatically treated using a combination of *ThCel7B*, *TcXyn10A* and *TtLPMO9H* at an enzyme loading of 1 mg of each enzyme per g of substrate (dry weight). To promote LPMO activity, 1 mM of ascorbic acid (electron donor) was added to the reaction medium. Reaction was carried out in 50 mM acetate buffer (pH 5) with a solid concentration of 1 % (w/v), incubated at 50 °C under stirring, for 3 and 24 h, resulting in samples hereafter called EN-CNF3 and EN-CNF24. A control reaction using pretreated samples, without enzymes or TEMPO-oxidation, was performed in parallel.

After the enzymatic treatment, samples were heated to 95 °C for 15 min to denature the enzymes and stop the reaction. Next, the solid material was separated from the supernatant and the solid fraction was washed with 0.1 M HCl and with distilled water for several times until reaching neutral pH. Then, samples EN-CNF3 and EN-CNF24 were both redispersed in 15 mL deionized water and nanofibrillated via ultrasonication using a Branson Ultrasonics Sonifier<sup>TM</sup> (Digital Sonifier 250 W) equipped with a 3.2-mm-diameter tapered microtip at 30 % of amplitude for 20 min. The resulting samples of cellulose nanofibers were stored in a refrigerator at 4 °C for further analyses.

### 2.5. Nanofibrillation by TEMPO-oxidation

First, 2 g of pretreated SCB was suspended in 150 mL of distilled water, and TEMPO (2,2,6,6-tetramethylpiperidine-1-oxyl) (0.025 g) and NaBr (0.25 g) were added to the mixture, which was kept under magnetic stirring at a room temperature. Next, 19.4 mmol/g of NaClO<sub>2</sub> solution (0.13 L, pH 10) was slowly added to the mixture, while maintaining pH at 10.5 by the addition of a 0.5 M NaOH solution. After 2 h, no further change in pH was observed, indicating the end of the reaction (Fukuzumi, Saito, Okita, & Isogai, 2010). The resulting solution was then filtered, washed and suspended in water. The suspension was finally sonicated using the same conditions (30 % amplitude for 20 min) previously applied to enzymatically treated samples to obtain a dispersion of nanofibers (TO-CNF).

Cellulose nanofibers from both enzymatic and TEMPO-oxidation pretreatments were dried at 35 °C for two days to obtain films that were characterized by X-ray diffraction (XRD) and thermogravimetric analysis (TGA).

### 2.6. X-ray diffraction (XRD)

XRD data from CNF films obtained with and without enzymatic pretreatments were collected using Cu K $\alpha$  radiation ( $\lambda = 1.5406 \text{ \AA}$ ) on a Rigaku Miniflex 600 X-ray diffractometer operating at 40 kV and 15 mA. Detection was carried out in the 2 $\theta$  range from 5 to 60°, with a step

interval of 0.05° and 15 s of exposure per step. Deconvolution was performed with PeakFit® 4.12 software assuming previously established procedures (Bernardinelli, Lima, Rezende, Polikarpov, & De Azevedo, 2015; Brar et al., 2020; Park, Baker, Himmel, Parilla, & Johnson, 2010). The crystallinity index (CrI) following the deconvolution method was determined by Eq. (1):

$$CrI = \frac{A_{cryst}}{A_{total}} \times 100 \quad (1)$$

where  $A_{cryst}$  = sum of deconvoluted crystalline band areas; and  $A_{total}$  = total area under the diffractogram (Bernardinelli et al., 2015).

The crystallite sizes (D) were calculated using Scherrer equation (Langford & Wilson, 1978) given below:

$$D = \frac{K\lambda}{\beta \cos\theta} \quad (2)$$

Here K is the correction factor (0.9),  $\lambda$  is the wavelength of the X-ray radiation (1.54056 Å),  $\beta$  is the full width at half maximum of the diffraction peak in radians, and  $\theta$  is the diffraction angle.

### 2.7. Content of oxidized groups

The carboxylic acid groups of the cellulose nanofibers produced with and without enzymatic or TEMPO pretreatments were measured using the conductometric method as described by Foster et al. (2018).

### 2.8. Scanning electron microscopy (SEM)

CNF samples were imaged using a scanning electron microscope DSM 960 (Zeiss, Oberkochen, Germany). 10  $\mu$ L of a CNF suspension (concentration of 0.01 % w/v) were dropped on a previously cleaned silicon surface. After drying, samples were coated with a thin layer of Au in a SCD 050 sputter coater (Oerlikon-Balzers, Balzers, Liechtenstein). Nanofiber diameters were determined by width measurements of a total of 30 nanofibers per sample and image analyses were performed using ImageJ software.

### 2.9. Atomic force microscopy (AFM)

AFM images were obtained in the Bruker Multimode 8 equipment, in tapping mode, using silicon tips (FMR NanoWorld), with cantilever spring constant of 2.8 N/m and nominal resonance of 75 kHz. Samples were dispersed in MilliQ water to obtain a final concentration of 5 mg/L (0.0005 % w/v). Then, the dispersions were sonicated for 2 min using an ultrasonication system at 130 W and 40 % of amplitude in pulsed mode (30 s on and 30 s off) for homogenization. The dispersions were dropped in cleaved mica supports previously modified with 10  $\mu$ L L-lysine and dried by natural evaporation. CNF diameters (250–430 nanofibers measured per sample) and lengths (170–380 nanofibers measured per sample) were determined using the software Gwyddion 2.54.

### 2.10. Thermogravimetric analysis (TGA)

Thermogravimetric analyses (TGA) were performed using a STA 409C – NETZSCH equipment, varying temperature from room temperature to 600 °C at a heating rate of 10 °C min<sup>-1</sup> under a nitrogen atmosphere (10 mL min<sup>-1</sup> flow).

## 3. Results and discussion

### 3.1. Chemical composition of sugarcane bagasse

The role of pretreatments of sugarcane bagasse is to decrease the contents of lignin, ash and hemicellulose, aiming to obtain a substrate enriched in cellulose and more prone to fibrillation. Table 1 shows the

**Table 1**

Chemical composition of sugarcane bagasse (SCB) before and after pretreatment.

	Untreated SCB	Pretreated SCB
Cellulose (%)	37.8 ± 0.1	74.8 ± 3.8
Hemicellulose (%)	22.2 ± 0.2	12.8 ± 1.6
Lignin (%)	21.1 ± 1.0	2.0 ± 0.6
Ashes (%)	5.2 ± 1.1	0.6 ± 0.1
Extractives (%)	12.0 ± 0.7	–
Total (%)	98.3 ± 3.1	90.2 ± 6.0
Solid Recovery (%)	–	52.4 ± 2.8

chemical composition of SCB biomass, before and after the applied pretreatments, revealing that the amount of lignin strongly decreased, from 21.7 ± 1.0 % in the untreated bagasse to 2 ± 0.6 % after the pretreatment. As a consequence, the cellulose content increased from 44.5 ± 0.2%–74.8 ± 3.8 % in the pretreated samples, thus indicating that the applied two-step pretreatment was effective in delignifying the sample and in increasing its cellulose content for consecutive nanofibrillation. Although the amount of hemicellulose was relatively high in the pretreated sample (12.8 ± 1.6 %), this was not a concern considering that xylanase was one of the enzymes used in the following step. Furthermore, extractives from pretreated SCB were not determined after pretreatment because they were assumed to be removed in the process. Although alternating KOH and NaClO treatments is a quite water-consuming procedure, this pretreatment protocol was efficient to prepare SCB substrates for nanofibrillation. Although a truly superior solution of water consumption is still a matter of debate, less water-demanding techniques, such as the ones described in Perzon, Jørgensen, and Ulvskov (2020) can be considered in a future work to at least partially address this issue.

### 3.2. Morphology of the nanofibers

SEM analysis of the control samples, prepared by defibrillation using ultrasound in the absence of enzymes or TEMPO, is given in Fig. 1a. An average diameter of CNF obtained by this method is 43 nm (Fig. 1d), indicating that the use of ultrasound alone has already provided enough energy to defibrillate the cellulose fibers until reaching a diameter in the nanometer scale. This agrees with previous results obtained on ultrasonic defibrillation of wood cellulose (wood powder from poplar trees), which was pretreated following very similar protocols as the ones used in the current study, though applying longer ultrasonication time (Chen et al., 2011).

SEM images of the enzymatically treated samples EN-CNF3 and EN-CNF24 are shown in Fig. 1b and c. The average diameter estimated for CNF samples obtained after 3 h of reaction was 28 nm (Fig. 1e), while enzymatic treatment for 24 h led to samples with an average diameter of 31 nm (Fig. 1f). The apparent CNF diameters are similar most probably because the samples were subjected to metallization prior to SEM analyses (Foster et al., 2018). Diameter measurements using AFM images are more realistic since they are based on fiber topography and AFM imaging does not require metallization.

As a next step, to compare CNF obtained by the traditional TEMPO-oxidation with those obtained by enzymatic action, AFM topography images of samples EN-CNF3, EN-CNF24 and TO-CNF were obtained (Fig. 2). The differences between these samples are very clear, with thinner and shorter fiber resulting from TEMPO reaction (Fig. 2a) and very long fibers obtained by the enzymatic hydrolysis (Fig. 2b). Fig. 2b and c allow comparison between different hydrolysis times (3 and 24 h), where the incomplete fibrillation of some fiber bundles in sample EN-CNF3 can be noticed. The fiber lengths measured in AFM images were distributed between 60 and 1820 nm in TEMPO-oxidized samples, with an average value of 400 ± 200 nm. In contrast, much longer CNF were obtained in sample EN-CNF24, with many fiber lengths exceeding the limits of the image (image size of 5  $\mu$ m). By measuring only the fibers

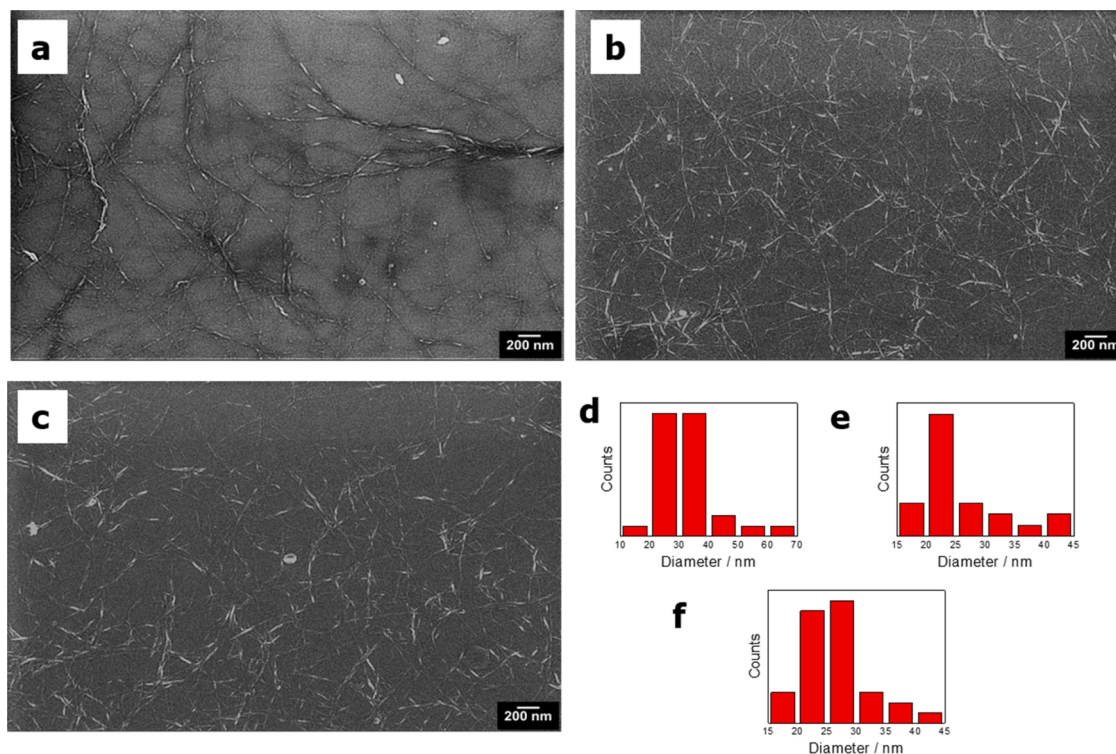


Fig. 1. Images obtained by SEM of (a) control, (b) EN-CNF3 and (c) EN-CNF24, with their respective fiber width distributions in (d), (e) and (f).

with identifiable ends within the image area, lengths varying from 188 nm to 5.3  $\mu\text{m}$  were identified, with an average length of  $1.3 \pm 0.9 \mu\text{m}$ . Noteworthy, the fiber length values of sample EN-CNF24 are certainly underestimated, as can be observed in Fig. 2.

The samples shown in Fig. 2 provide a good basis for comparison since they came from the same biomass source (SCB) and underwent identical delignification, bleaching and sonication protocols. The only difference between these samples is that TEMPO-oxidation step (Fig. 2a) was replaced by the enzymatic hydrolysis for enzymatically treated samples (Fig. 2b and c). Longer CNF were isolated from sugarcane bagasse ( $605 \pm 170 \text{ nm}$ ) after TEMPO oxidation in a previous work (Pinto et al., 2019), but using distinct delignification, bleaching and sonication conditions. Saito, Kimura, Nishiyama, and Isogai (2007) also obtained longer TEMPO-oxidized CNF (few micrometers in length), but from a different biomass source (hardwood), and delignified and bleached differently (bleached hardwood Kraft pulp). Furthermore, these CNFs were obtained by a distinct fibrillation method (magnetic stirring).

In terms of nanofiber diameters, the enzymatically treated samples (EN-CNF24) have diameters from 1.3–20 nm, with an average value of  $7 \pm 3 \text{ nm}$  (Fig. 2d). According to the values published in the literature for cellulose elementary fibrils (1.5–3.5 nm), Fig. 2b contains CNF that are formed by no more than one elementary fibril, but also thicker CNF, formed by bundles of a few elementary fibrils (Zhu, Fang, Preston, Li, & Hu, 2014). On the other hand, TO-CNF are thinner, with diameters distributed in a smaller range (between 0.7 and 7.6 nm, with an average diameter of  $3 \pm 1 \text{ nm}$ , Fig. 2d). These results are in agreement with the higher degree of oxidation reached in TEMPO-oxidized samples, which increases electrostatic repulsion between fibers, facilitating disaggregation and the fibrillation process. Therefore, the impressive fiber lengths in the  $\mu\text{m}$  scale, associated to diameters in the nanometer scale observed for enzymatically produced CNFs highlight the clear differences between enzymatic and chemical routes for CNF production.

Based on our estimates of enzymatic hydrolysis yields, less than 5% and 7% of the cellulose fraction has been hydrolyzed after 3 h and 24 h of reaction, respectively. Therefore, the enzymatic treatment should not

lead to a significant reduction in the yields of CNF production. Furthermore, efficiency of hydrolysis can be optimized by choosing advanced enzymatic mixtures and adjusting their doses and reaction times.

Our results suggest that the combined treatment using enzymes and mechanical action on SCB provided nanofibers with higher aspect ratio (length/diameter) than nanofibers resulting from chemical (TEMPO-oxidation) and mechanical treatment. A similar feature was reported by Henriksson, Henriksson, Berglund, and Lindström (2007), where the AFM images of a combination of PFI-mill action and enzyme treatment (using an endoglucanase) showed cellulose nanofibers from commercial bleached wood sulfite pulps with higher aspect ratio than nanofibers resulting from fibers subjected to hydrolysis by a strong acid. Bian, Li, Jiao, Yu, and Dai (2016) also reported that CNFs from bleached spruce kraft pulp subjected to enzymatic treatment, performed with a laccase and a xylanase, combined with homogenization had larger aspect ratio than those from pure mechanical treatment.

The high aspect ratio of enzymatically treated CNFs is a highly desirable characteristic, mainly for applications which are intended to improve the mechanical properties of a final product (Kargarzadeh et al., 2017). For this reason, cellulose nanofibers have been extensively incorporated into plastics to improve strength and decrease costs (Jonoobi, Harun, Mathew, & Oksman, 2010; Klemm et al., 2011). Furthermore, some studies investigate their potential as rheological modifiers in bulk applications (Lowys, Desbrières, & Rinaudo, 2001; Pääkko et al., 2007).

### 3.3. Crystallinity of cellulose nanofibers

We assessed and compared the crystallinity indices (CIs) for all the samples, but no significant differences were observed between enzymatically treated and non-enzymatically treated groups (Fig. 3a). Although EN-CNF24 has somewhat lower CI as compared with EN-CNF3 ( $65 \pm 1\%$  and  $72 \pm 3\%$ , respectively), they were not significantly different from control and TO-CNF samples. This might indicate that chemical pretreatment and mechanical defibrillation steps were

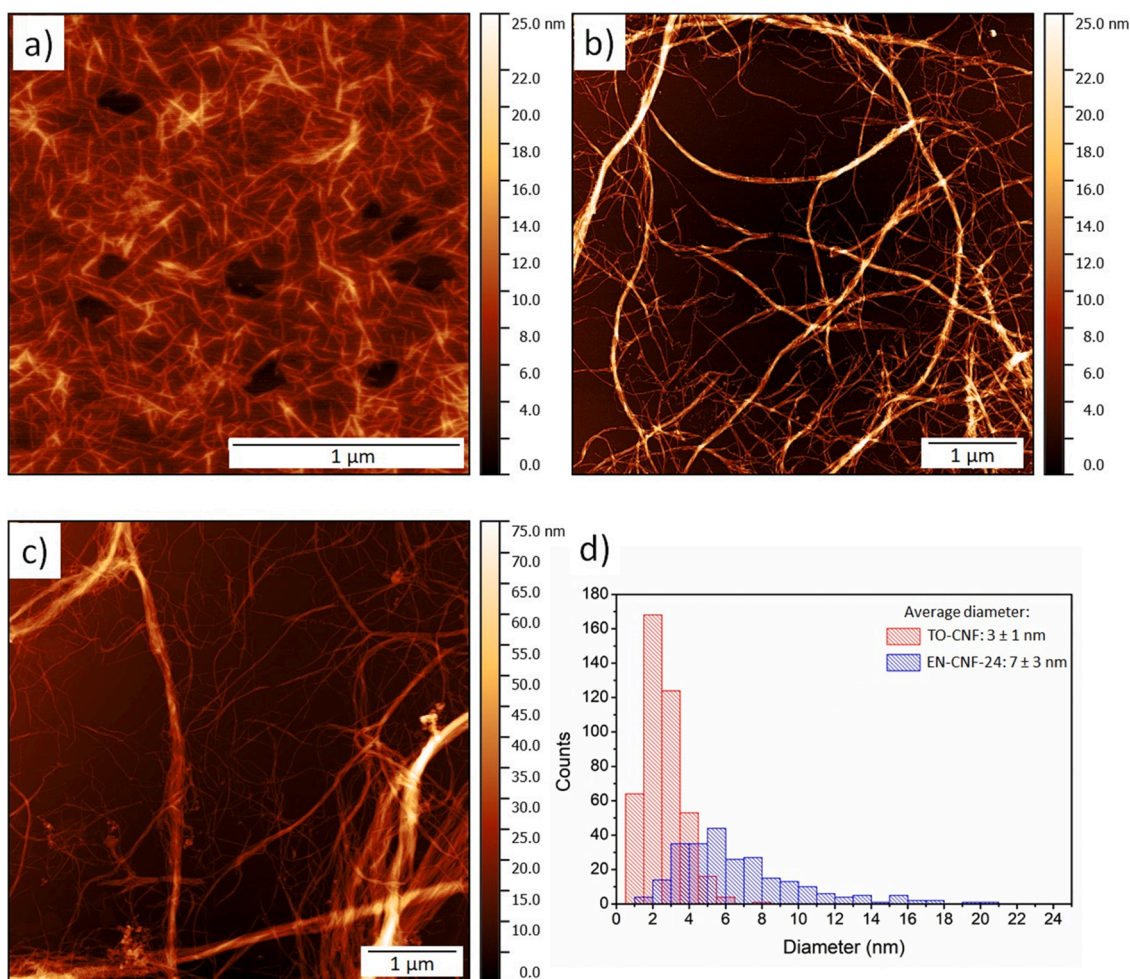


**Fig. 2.** AFM topography images of samples treated by (a) TEMPO-oxidation (TO-CNF); (b) enzymes for 3 h (EN-CNF3) and (c) 24 h (EN-CNF24); (d) histograms of diameter distribution for samples TO-CNF and EN-CNF24.

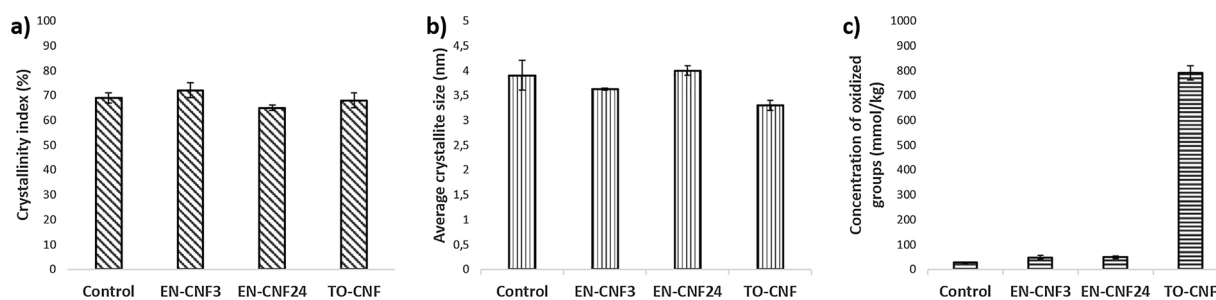


**Fig. 3.** Crystallinity and oxidation of the obtained CNF. a) Crystallinity indexes, b) average crystal sizes and c) concentration of the oxidized groups for control samples, EN-CNF3, EN-CNF24 and TO-CNF.

predominant in defining the crystallinities of the final CNFs. CIs of the CNF samples obtained in the absence of enzymes agree well with those determined for wood cellulose CNF (Chen et al., 2011).

On the other hand, the average crystallite sizes for TEMPO-oxidized samples were significantly different from both non-oxidized control samples and enzymatically treated EN-CNF3 and EN-CNF24 (Fig. 3b). The changes in average crystal sizes of CNF could be associated to a removal of amorphous hemicellulose and lignin fractions as a result of applied chemical treatments of the biomass and a consequent recrystallization of cellulose fibrils into larger crystallites (Driemeier, Mendes, Santucci, & Pimenta, 2015). Significantly stronger oxidation of cellulose by TEMPO (Fig. 3c) leading to introduction of negative charges on the

surface of the cellulose fibrils would partially prevent collapse and recrystallization of the oxidized cellulose fibrils, which is consistent with smaller average crystallite sizes for TO-CNF samples determined from DRX experiments (Fig. 3b). Conversely, limited enzymatic hydrolysis under conditions of our experiments and milder oxidation promoted by LPMO resulted in large crystallites which were similar in size to the ones in non-oxidized control samples (Fig. 3b).

#### 3.4. Concentration of oxidized groups in cellulose nanofibers

Oxidative action of the TrLPMO9H promoted significant increase in the oxidation of the fibers (Fig. 3c). Indeed, the concentration of

oxidized groups in samples EN-CNF3 and EN-CNF24 is 2 times higher as compared to the samples prepared in the absence of the enzymes or of TEMPO-oxidation (control). Samples EN-CNF3 and EN-CNF24 showed no significant difference in concentration of oxidized groups between them, despite the difference in the reaction times. According to Hu et al. (2018), the enzymatic action of LPMOs on cellulosic materials promotes the oxidation and removal of cellulose outermost layers, exposing inner layers with similar characteristics, but that have not yet undergone any enzymatic oxidation. The enzymes continue acting on the newly exposed layers and the process goes on and on. This might explain the same concentration of oxidized groups between EN-CNF3 and EN-CNF24, which might correspond to a maximum apparent concentration of oxidized groups introduced into the surface of pretreated SCB by the mixture of enzymes. The concentrations of oxidized groups in the samples were consistent with the number of oxidative groups introduced by LPMO treatment in previous studies (~100 mmol/kg substrate; Hu et al., 2018).

TEMPO oxidation was significantly more efficient in introducing oxidized groups into pretreated SCB (Fig. 3c), in agreement with other studies that used TEMPO for cellulose oxidation (Isogai, Saito, & Fukuzumi, 2011; Wei et al., 2016). At the same time, the concentration of carboxylic groups introduced under the experimental conditions applied herewith was close to the lower limit of the range achieved in previously studies (800~1500 mmol/kg substrate; Rol et al., 2019; Saito et al., 2007), indicating that TEMPO was much more efficient than LPMO in cellulose oxidation.

### 3.5. Thermostability analysis of nanocellulose fibers

It is widely recognized that thermostability is a desirable feature for a number of engineering applications, such as, for example, the production of electronic components, which have to maintain their stability under highly variable temperature regimes. The preparation of polymer nanocomposites by extrusion or injection molding also requires thermally stable fillers to be incorporated into the polymer matrix. However, earlier studies (Qua, Hornsby, Sharma, & Lyons, 2011; Yang et al., 2017) demonstrated that many of the chemical pretreatment processes used to promote cellulose fibrillation led to a reduced thermostability of the resulting fibers.

Thermostability of the CNF obtained in this work was analyzed by thermogravimetric analysis (TGA). TGA and differential thermogravimetry (DTG) curves are shown in Fig. 4a and b, while initial decomposition temperature ( $T_{\text{onset}}$ ) and temperature of maximum weight loss ( $T_{\text{max}}$ ) are given in Table 2. The weight loss of TO-CNF (Fig. 4) is quite different from the profile observed in all the other samples (both enzymatically treated and the control). TO-CNF showed a broad thermal degradation, with two events of weight loss, while the

**Table 2**

Initial decomposition temperature ( $T_{\text{onset}}$ ) and temperature of maximum weight loss ( $T_{\text{max}}$ ) of nanocellulosic fibers after 3 and 24-h of enzymatic reactions, control or TEMPO oxidation reaction, obtained via TGA.

Sample	$T_{\text{onset}}$ (°C)	$T_{\text{max}}$ (°C)
EN-CNF3	273 ± 6	316 ± 6
EN-CNF24	261 ± 7	315 ± 5
Control	272 ± 7	317 ± 3
TO-CNF	193 ± 8 (peak 1)	249 ± 4 (peak 1)
	290 ± 5 (peak 2)	308 ± 5 (peak 2)

enzymatically treated samples (EN-CNF3 and EN-CNF 24) had only one degradation peak in a profile very similar to the control (pretreated and bleached cellulose fibers).

Furthermore, TO-CNF is less stable than the other samples, with decomposition starting at 193 °C and with two degradation peaks with maximums at  $T_{\text{max}(1)} = 249$  and  $T_{\text{max}(2)} = 308$  °C (Table 2). Differently, sample EN-CNF24 starts to degrade at 261 °C, with maximum degradation at 315°. The results obtained from CNF produced using TEMPO oxidation were very similar to other studies reported in the literature on the cellulose chemical treatments with TEMPO (El Bakkari, Bindiganavile, Goncalves, & Boluk, 2019; Fukuzumi, Saito, Iwata, Kumamoto, & Isogai, 2009). The reduced stability of the samples can be explained by the introduction of sodium carboxylate groups in TO-CNF during TEMPO-mediated oxidation, which leads to decarbonation during heating process and decreases the thermal stability (Fukuzumi et al., 2010; Yang et al., 2017; Zhao, Moser, Lindström, Henriksson, & Li, 2017). Though the enzyme-induced oxidation promoted by LPMOs also inserts carboxylate groups at the cellulose surface, insertions occur at C1 and/or C4 positions. Quite differently, TEMPO treatment inserts carboxyl group at C6 carbon position (Hu et al., 2018; Isogai et al., 2011; Westereng et al., 2016). Thus, the differences observed in Fig. 4 are presumably associated with the different nature of the applied pretreatments.

The resulting material obtained by enzymatic treatment has higher thermostability when compared with nanofibers produced via the more traditional chemical route, using TEMPO-oxidation. Similar results were reported by Martelli-Tosi et al. (2018) that used an enzymatic cocktail (composed of an endoglucanase and a xylanase), followed by mechanical homogenization to produce CNF from soybean straw. The authors obtained nanofibrillated cellulose with higher aspect ratio and greater thermal stability as compared to nanocellulose obtained by acid hydrolysis (Martelli-Tosi et al., 2018).

## 4. Conclusions

The cooperative action of a set of recombinant enzymes (an

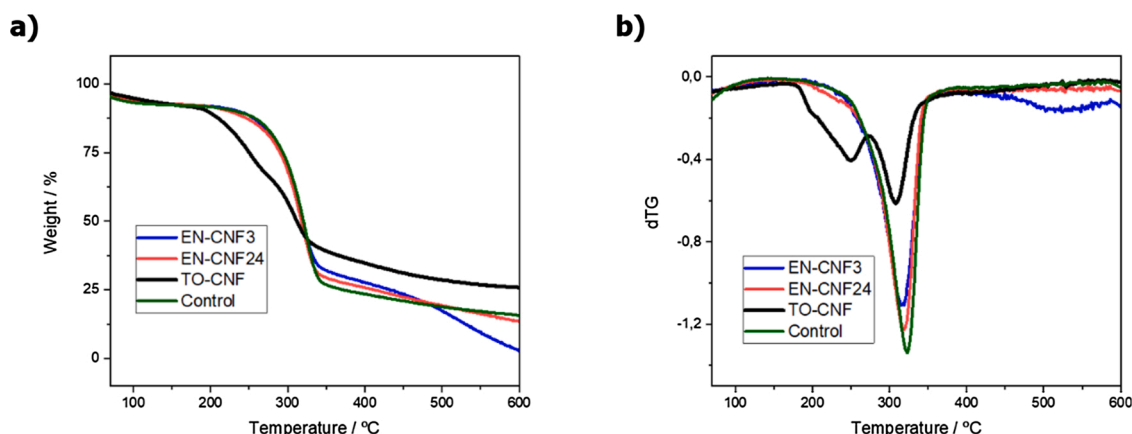


**Fig. 4.** (a) Thermogravimetric (TG) and (b) Differential thermogravimetric (DTG) curves of EN-CNF3, EN-CNF24, TO-CNF and control samples.

endoglucanase, a xylanase and a LPMO) followed by sonication allowed the preparation of cellulose nanofibrils from sugarcane bagasse, which are much longer and more thermostable (resisting up to 260° for the initial degradation temperature) as compared to the analogous CNF prepared by TEMPO-mediated oxidation. For applications where high temperature is a key issue (e.g. electronic components and molded nanocomposites), the use of materials with higher thermostability is highly desirable and thus enzymatic route for CNF production could be preferable. Furthermore, significantly longer enzymatically produced CNF may also be attractive for applications in packaging and as reinforcing and rheology modifier agents.

#### CRedit authorship contribution statement

**Bruno R. Rossi:** Investigation, Formal analysis, Data curation, Writing - original draft. **Vanessa O.A. Pellegrini:** Investigation, Formal analysis, Data curation, Writing - original draft, Writing - review & editing, Project administration. **Anelyse A. Cortez:** Investigation, Formal analysis, Visualization, Writing - original draft, Writing - review & editing. **Emanuele M.S. Chiromito:** Investigation, Formal analysis. **Antonio J.F. Carvalho:** Conceptualization, Methodology, Supervision. **Lidiane O. Pinto:** Investigation, Formal analysis, Visualization, Writing - original draft, Writing - review & editing. **Camila A. Rezende:** Investigation, Formal analysis, Visualization, Writing - original draft, Writing - review & editing, Supervision. **Valmor R. Mastelaro:** Conceptualization, Methodology, Writing - original draft, Supervision. **Igor Polikarpov:** Conceptualization, Methodology, Writing - original draft, Writing - review & editing, Supervision, Funding acquisition.

#### Acknowledgements

This research was supported by Fundação de Amparo à Pesquisa do Estado de São Paulo (FAPESP) (grants 2015/13684-0 and 2018/23769-1) and by Conselho Nacional de Desenvolvimento Científico e Tecnológico (CNPq) (grants 423693/2016-6 and 303988/2016-9).

#### References

- Bernardes, A., Pellegrini, V. O. A., Curtolo, F., Camilo, C. M., Mello, B. L., Johns, M. A., ... Polikarpov, I. (2019). Carbohydrate binding modules enhance cellulose enzymatic hydrolysis by increasing access of cellulases to the substrate. *Carbohydrate Polymers*, 211, 57–68. <https://doi.org/10.1016/j.carbpol.2019.01.108>
- Bernardinelli, O. D., Lima, M. A., Rezende, C. A., Polikarpov, I., & De Azevedo, E. R. (2015). Quantitative <sup>13</sup>C MultiCP solid-state NMR as a tool for evaluation of cellulose crystallinity index measured directly inside sugarcane biomass. *Biotechnology for Biofuels*, 8(1), 1–11. <https://doi.org/10.1186/s13068-015-0292-1>
- Bian, H., Dong, M., Chen, L., Zhou, X., Ni, S., Fang, G., ... Dai, H. (2019). Comparison of mixed enzymatic pretreatment and post-treatment for enhancing the cellulose nanofibrillation efficiency. *Bioresour Technol*, 293(September). <https://doi.org/10.1016/j.biortech.2019.122171>
- Bian, H., Li, G., Jiao, L., Yu, Z., & Dai, H. (2016). Enzyme-assisted mechanical fibrillation of bleached spruce kraft pulp for producing well-dispersed and uniform-sized cellulose nanofibrils. *BioResources*, 11(4), 10483–10496. <https://doi.org/10.15376/biores.11.4.10483-10496>
- Blanco, A., Monte, M. C., Campano, C., Balea, A., Merayo, N., & Negro, C. (2018). Nanocellulose for industrial use: Cellulose nanofibers (CNF), cellulose nanocrystals (CNC), and bacterial cellulose (BC). *Handbook of nanomaterials for industrial applications*. <https://doi.org/10.1016/B978-0-12-813351-4.00005-5>
- Brar, K. K., Espirito Santo, M. C., Pellegrini, V. O. A., De Azevedo, E. R., Guimaraes, F. E. C., Polikarpov, I., ... Chadha, B. S. (2020). Enhanced hydrolysis of hydrothermally and autohydrolytically treated sugarcane bagasse and understanding the structural changes leading to improved saccharification. *Biomass & Bioenergy*, 139(May 2019), Article 105639. <https://doi.org/10.1016/j.biombioe.2020.105639>
- Chen, W., Yu, H., Liu, Y., Chen, P., Zhang, M., & Hai, Y. (2011). Individualization of cellulose nanofibers from wood using high-intensity ultrasonication combined with chemical pretreatments. *Carbohydrate Polymers*, 83(4), 1804–1811. <https://doi.org/10.1016/j.carbpol.2010.10.040>
- Companhia Nacional do Abastecimento (CONAB). (2020). *Acompanhamento da Safra Brasileira: cana-de-açúcar*. Retrieved April 8, 2020, from COMPANHIA NACIONAL DO ABASTECIMENTO (CONAB). website: <https://portaldeinformacoes.conab.gov.br/safras/ca>.
- de Campos, A., Correa, A. C., Cannella, D., de M Teixeira, E., Marconcini, J. M., Dufresne, A., ... Sanadi, A. R. (2013). Obtaining nanofibers from curauá and sugarcane bagasse fibers using enzymatic hydrolysis followed by sonication. *Cellulose*, 20(3), 1491–1500. <https://doi.org/10.1007/s10570-013-9909-3>
- De France, K. J., Hoare, T., & Cranston, E. D. (2017). Review of hydrogels and aerogels containing nanocellulose. *Chemistry of Materials*, 29(11), 4609–4631. <https://doi.org/10.1021/acs.chemmater.7b00531>
- Drimeier, C., Mendes, F. M., Santucci, B. S., & Pimenta, M. T. B. (2015). Cellulose crystallization and related phenomena occurring in hydrothermal treatment of sugarcane bagasse. *Cellulose*, 22, 2183–2195. <https://doi.org/10.1007/s10570-015-0638-7>
- Dufresne, A. (2019). Nanocellulose processing properties and potential applications. *Current Forestry Reports*, 5, 76–89. <https://doi.org/10.1007/s40725-019-00088-1>
- El Bakkari, M., Bindiganavile, V., Goncalves, J., & Boluk, Y. (2019). Preparation of cellulose nanofibers by TEMPO-oxidation of bleached chemi-thermomechanical pulp for cement applications. *Carbohydrate Polymers*, 203, 238–245. <https://doi.org/10.1016/j.carbpol.2018.09.036>
- Errokh, A., Magnin, A., Putaux, J. L., & Boufi, S. (2018). Morphology of the nanocellulose produced by periodate oxidation and reductive treatment of cellulose fibers. *Cellulose*, 25(7), 3899–3911. <https://doi.org/10.1007/s10570-018-1871-7>
- Espirito Santo, M., Rezende, C. A., Bernardinelli, O. D., Pereira, N., Curvelo, A. A. S., deAzevedo, E. R., ... Polikarpov, I. (2018). Structural and compositional changes in sugarcane bagasse subjected to hydrothermal and organosolv pretreatments and their impacts on enzymatic hydrolysis. *Industrial Crops and Products*, 113(December 2017), 64–74. <https://doi.org/10.1016/j.indcrop.2018.01.014>
- Evangelista, D. E., de Oliveira, A., Pellegrini, V., Santo, M. E., McQueen-Mason, S., Bruce, N. C., ... Polikarpov, I. (2019). Biochemical characterization and low-resolution SAXS shape of a novel GH11 exo-1,4-β-xylanase identified in a microbial consortium. *Applied Microbiology and Biotechnology*, 103(19), 8035–8049. <https://doi.org/10.1007/s00253-019-10033-8>
- Farinas, C. S., Marconcini, J. M., & Mattoso, L. H. C. (2018). Enzymatic conversion of sugarcane lignocellulosic biomass as a platform for the production of ethanol, enzymes and nanocellulose. *Journal of Renewable Materials*, 6(2), 203–216. <https://doi.org/10.7569/JRM.2017.6341578>
- Foster, E. J., Moon, R. J., Agarwal, U. P., Bortner, M. J., Bras, J., Camarero-Espinosa, S., ... Youngblood, J. (2018). Current characterization methods for cellulose nanomaterials. *Chemical Society Reviews*, 47(8), 2609–2679. <https://doi.org/10.1039/C6CS00895J>
- Fukuzumi, H., Saito, T., Iwata, T., Kumamoto, Y., & Isogai, A. (2009). Transparent and high gas barrier films of cellulose nanofibers prepared by TEMPO-mediated oxidation. *Biomacromolecules*, 10(1), 162–165. <https://doi.org/10.1021/bm801065u>
- Fukuzumi, H., Saito, T., Okita, Y., & Isogai, A. (2010). Thermal stabilization of TEMPO-oxidized cellulose. *Polymer Degradation and Stability*, 95, 1502–1508. <https://doi.org/10.1016/j.polymerdegradstab.2010.06.015>
- Gouveia, E. R., do Nascimento, R. T., Souto-Maior, A. M., & de M. Rocha, G. J. (2009). Validação de metodologia para a caracterização química de bagaço de cana-de-açúcar. *Química Nova*, 32(6), 1500–1503.
- Grande, R., Trovatti, E., Pimenta, M. T. B., & Carvalho, A. J. F. (2018). Microfibrillated cellulose from sugarcane bagasse as a biorefinery product for ethanol production. *Journal of Renewable Materials*, 6(2), 195–202. <https://doi.org/10.7569/JRM.2018.634109>
- Habibi, Y., Lucia, L. A., & Rojas, O. J. (2010). Cellulose nanocrystals: Chemistry, self-assembly, and applications. *Chemical Reviews*, 110(6), 3479–3500. <https://doi.org/10.1021/cr900339w>
- Henriksson, M., Henriksson, G., Berglund, L. A., & Lindström, T. (2007). An environmentally friendly method for enzyme-assisted preparation of microfibrillated cellulose (MFC) nanofibers. *European Polymer Journal*, 43(8), 3434–3441. <https://doi.org/10.1016/j.eurpolymj.2007.05.038>
- Hu, J., Arantes, V., Pribowo, A., Gourlay, K., & Saddler, J. N. (2014). Substrate factors that influence the synergistic interaction of AA9 and cellulases during the enzymatic hydrolysis of biomass. *Energy & Environmental Science*, 7(7), 2308–2315. <https://doi.org/10.1039/C4EE00891J>
- Hu, J., Arantes, V., & Saddler, J. N. (2011). The enhancement of enzymatic hydrolysis of lignocellulosic substrates by the addition of accessory enzymes such as xylanase: Is it an additive or synergistic effect? *Biotechnology for Biofuels*, 4(October). <https://doi.org/10.1186/1754-6834-4-36>
- Hu, J., Tian, D., Rennecker, S., & Saddler, J. N. (2018). Enzyme mediated nanofibrillation of cellulose by the synergistic actions of an endoglucanase, lytic polysaccharide monoxygenase (LPMO) and xylanase. *Scientific Reports*, 8(1), 4–11. <https://doi.org/10.1038/s41598-018-21016-6>
- Isogai, A., Saito, T., & Fukuzumi, H. (2011). TEMPO-oxidized cellulose nanofibers. *Nanoscale*, 3(1), 71–85. <https://doi.org/10.1039/c0nr00583e>
- Jonoobi, M., Harun, J., Mathew, A. P., & Oksman, K. (2010). Mechanical properties of cellulose nanofiber (CNF) reinforced poly(lactic acid) (PLA) prepared by twin screw extrusion. *Composites Science and Technology*, 70(12), 1742–1747. <https://doi.org/10.1016/j.compscitech.2010.07.005>
- Kadowaki, M. A. S., Várnai, A., Jameson, J. K., Leite, A. E. T., Costa-Filho, A. J., Kumagai, P. S., ... Eijsink, V. G. H. (2018). Functional characterization of a lytic polysaccharide monoxygenase from the thermophilic fungus *Myceliophthora thermophila*. *PLoS One*, 13(8), 1–16. <https://doi.org/10.1371/journal.pone.0202148>
- Kargazadeh, H., Mariano, M., Huang, J., Lin, N., Ahmad, I., Dufresne, A., ... Thomas, S. (2017). Recent developments on nanocellulose reinforced polymer nanocomposites: A review. *Polymer*, 132, 368–393. <https://doi.org/10.1016/j.polymer.2017.09.043>
- Keller, M. B., Badino, S. F., Blossom, B. M., McBrayer, B., Borch, K., & Westh, P. (2020). Promoting and impeding effects of lytic polysaccharide monoxygenases on glycoside hydrolase activity. *ACS Sustainable Chemistry & Engineering*, 8(37), 14117–14126. <https://doi.org/10.1021/acscuschemeng.0c04779>

- Klemm, D., Cranston, E. D., Fischer, D., Gama, M., Kedzior, S. A., Kralisch, D., ... Rauchfuß, F. (2018). Nanocellulose as a natural source for groundbreaking applications in materials science: Today's state. *Materials Today*, 21(7), 720–748. <https://doi.org/10.1016/j.matod.2018.02.001>
- Klemm, D., Kramer, F., Moritz, S., Lindström, T., Ankerfors, M., Gray, D., ... Dorris, A. (2011). Nanocelluloses: A new family of nature-based materials. *Angewandte Chemie - International Edition*, 50(24), 5438–5466. <https://doi.org/10.1002/anie.2011001273>
- Koskela, S., Wang, S., Xu, D., Yang, X., Li, K., Berglund, L. A., ... Zhou, Q. (2019). Lytic polysaccharide monoxygenase (LPMO) mediated production of ultra-fine cellulose nanofibres from delignified softwood fibres. *Green Chemistry*, 21(21), 5924–5933. <https://doi.org/10.1039/c9gc02808k>
- Langford, J. I., & Wilson, A. J. C. (1978). Scherrer after sixty years: A survey and some new results in the determination of crystallite size. *Journal of Applied Crystallography*, 11, 102–113. <https://doi.org/10.1107/S0021889878012844>
- Lin, N., & Dufresne, A. (2014). Nanocellulose in biomedicine: Current status and future prospect. *European Polymer Journal*, 59, 302–325. <https://doi.org/10.1016/j.eurpolymj.2014.07.025>
- Liu, L., Kerr, W. L., & Kong, F. (2019). Characterization of lipid emulsions during in vitro digestion in the presence of three types of nanocellulose. *Journal of Colloid and Interface Science*, 545, 317–329. <https://doi.org/10.1016/j.jcis.2019.03.023>
- Loose, J. S. M., Forsberg, Z., Fraaije, M. W., Eijssink, V. G. H., & Vaaje-kolstad, G. (2014). A rapid quantitative activity assay shows that the *Vibrio cholerae* colonization factor GbpA is an active lytic polysaccharide monoxygenase. *FEBS Letters*, 588(18), 3435–3440. <https://doi.org/10.1016/j.febslet.2014.07.036>
- Lowys, M. P., Desbrières, J., & Rinaudo, M. (2001). Rheological characterization of cellulosic microfibril suspensions. Role of polymeric additives. *Food Hydrocolloids*, 15(1), 25–32. [https://doi.org/10.1016/S0268-005X\(00\)00046-1](https://doi.org/10.1016/S0268-005X(00)00046-1)
- Mandal, A., & Chakraborty, D. (2011). Isolation of nanocellulose from waste sugarcane bagasse (SCB) and its characterization. *Carbohydrate Polymers*, 86(3), 1291–1299. <https://doi.org/10.1016/j.carbpol.2011.06.030>
- Martelli-Tosi, M., Masson, M. M., Silva, N. C., Esposto, B. S., Barros, T. T., Assis, O. B. G., ... Tapia-Blácido, D. R. (2018). Soybean straw nanocellulose produced by enzymatic or acid treatment as a reinforcing filler in soy protein isolate films. *Carbohydrate Polymers*, 198(March), 61–68. <https://doi.org/10.1016/j.carbpol.2018.06.053>
- Ministério de Minas e Energia (MME). (2019). *Balanço Energético Nacional 2019*. Retrieved from <https://www.epe.gov.br/sites-pt/publicacoes-dados-abertos/publicacoes/PublicacoesArquivos/publicacao-377/topico-494/BEN2019CompletoWEB.pdf>
- Mokhena, T. C., & John, M. J. (2020). Cellulose nanomaterials: New generation materials for solving global issues. In *Cellulose* (Vol. 27). <https://doi.org/10.1007/s10570-019-02889-w>
- Moon, R. J., Martini, A., Nairn, J., Simonsen, J., & Youngblood, J. (2011). Cellulose nanomaterials review: Structure, properties and nanocomposites. *Chemical Society Reviews*, 40(7), 3941–3994. <https://doi.org/10.1039/c0cs00108b>
- Nechyporchuk, O., Belgacem, M. N., & Bras, J. (2016). Production of cellulose nanofibrils: A review of recent advances. *Industrial Crops and Products*, 93, 2–25. <https://doi.org/10.1016/j.indcrop.2016.02.016>
- Nie, S., Zhang, K., Lin, X., Zhang, C., Yan, D., Liang, H., ... Wang, S. (2018). Enzymatic pretreatment for the improvement of dispersion and film properties of cellulose nanofibrils. *Carbohydrate Polymers*, 181(November 2017), 1136–1142. <https://doi.org/10.1016/j.carbpol.2017.11.020>
- Oliveira, F. B., Bras, J., Pimenta, M. T. B., Curvelo, A. A. S., & Belgacem, M. N. (2016). Production of cellulose nanocrystals from sugarcane bagasse fibers and pith. *Industrial Crops and Products*, 93, 48–57. <https://doi.org/10.1016/j.indcrop.2016.04.064>
- Pääkko, M., Ankerfors, M., Kosonen, H., Nykänen, A., Ahola, S., Österberg, M., ... Lindström, T. (2007). Enzymatic hydrolysis combined with mechanical shearing and high-pressure homogenization for nanoscale cellulose fibrils and strong gels. *Biomacromolecules*, 8(6), 1934–1941. <https://doi.org/10.1021/bm061215p>
- Park, S., Baker, J. O., Himmel, M. E., Parilla, P. A., & Johnson, D. K. (2010). Cellulose crystallinity index: Measurement techniques and their impact on interpreting cellulase performance. *Biotechnology for Biofuels*, 1–10. <https://doi.org/10.1186/1754-6834-3-10>. Retrieved from.
- Park, Y., Doherty, W. O. S., & Halley, P. J. (2008). Developing lignin-based resin coatings and composites. *Industrial Crops and Products*, 27(2), 163–167. <https://doi.org/10.1016/j.indcrop.2007.07.021>
- Pellegrini, V. O. A., Bernardes, A., Rezende, C. A., & Polikarpov, I. (2018). Cellulose fiber size defines efficiency of enzymatic hydrolysis and impacts degree of synergy between endo- and exoglucanases. *Cellulose*, 25, 1865–1881. <https://doi.org/10.1007/s10570-018-1700-z>
- Pellegrini, V. O. A., Serpa, V. I., Godoy, A. S., Camilo, C. M., Bernardes, A., Rezende, C. A., ... Polikarpov, I. (2015). Recombinant *Trichoderma harzianum* endoglucanase I (Cel7B) is a highly acidic and promiscuous carbohydrate-active enzyme. *Applied Microbiology and Biotechnology*, 99(22), 9591–9604. <https://doi.org/10.1007/s00253-015-6772-1>
- Perzon, A., Jørgensen, B., & Ulvskov, P. (2020). Sustainable production of cellulose nanofiber gels and paper from sugar beet waste using enzymatic pre-treatment. *Carbohydrate Polymers*, 230, Article 115581. <https://doi.org/10.1016/j.carbpol.2019.115581>
- Phanthong, P., Reubroycharoen, P., Hao, X., Xu, G., Abudula, A., & Guan, G. (2018). Nanocellulose: Extraction and application. *Carbon Resources Conversion*, 1(1), 32–43. <https://doi.org/10.1016/j.crcon.2018.05.004>
- Pinto, L. O., Bernardes, J. S., & Rezende, C. A. (2019). Low-energy preparation of cellulose nanofibers from sugarcane bagasse by modulating the surface charge density. *Carbohydrate Polymers*, 218(April), 145–153. <https://doi.org/10.1016/j.carbpol.2019.04.070>
- Qua, E. H., Hornsby, P. R., Sharma, H. S. S., & Lyons, G. (2011). Preparation and characterisation of cellulose nanofibres. *Journal of Materials Science*, 46(18), 6029–6045. <https://doi.org/10.1007/s10853-011-5565-x>
- Ribeiro, R. S. A., Pohlmann, B. C., Calado, V., Bojorge, N., & Pereira, N. (2019). Production of nanocellulose by enzymatic hydrolysis: Trends and challenges. *Engineering in Life Sciences*, 19(4), 279–291. <https://doi.org/10.1002/elsc.201800158>
- Rocha, G. J., de, M., Silva, F. T., Curvelo, A. A., da, S., & Araujo, G. T. (1997). A fast and accurate method for determination of cellulose and polyoses by HPLC. *Brazilian Symposium on the Chemistry of Lignins and Other Wood Components*.
- Rol, F., Belgacem, M. N., Gandini, A., & Bras, J. (2019). Recent advances in surface-modified cellulose nanofibrils. *Progress in Polymer Science*, 88, 241–264. <https://doi.org/10.1016/j.progpolymsci.2018.09.002>
- Saele, K., Yingkamhaeng, N., Nimchua, T., & Sukyai, P. (2016). An environmentally friendly xylanase-assisted pretreatment for cellulose nanofibrils isolation from sugarcane bagasse by high-pressure homogenization. *Industrial Crops and Products*, 82, 149–160. <https://doi.org/10.1016/j.indcrop.2015.11.064>
- Saito, T., Kimura, S., Nishiyama, Y., & Isogai, A. (2007). Cellulose nanofibers prepared by TEMPO-mediated oxidation of native cellulose. *Biomacromolecules*, 8(8), 2485–2491. <https://doi.org/10.1021/bm0703970>
- Sepulchro, A. G. V., Pellegrini, V. O. A., Briganti, L., de Araujo, E. A., de Araujo, S. S., & Polikarpov, I. (2020). Transformation of xylan into value-added biocommodities using *Thermobacillus composti* GH10 xylanase. *Carbohydrate Polymers*, 247(July), Article 116714. <https://doi.org/10.1016/j.carbpol.2020.116714>
- Simmons, T. J., Frandsen, K. E. H., Ciano, L., Tryfona, T., Lenfant, N., Poulsen, J. C., ... Dupree, P. (2017). Structural and electronic determinants of lytic polysaccharide monoxygenase reactivity on polysaccharide substrates. *Nature Communications*, 8(1). <https://doi.org/10.1038/s41467-017-01247-3>
- Sonoda, M. T., Godoy, A. S., Pellegrini, V. O. A., Kadowaki, M. A. S., Nascimento, A. S., & Polikarpov, I. (2019). Structure and dynamics of *Trichoderma harzianum* Cel7B suggest molecular architecture adaptations required for a wide spectrum of activities on plant cell wall polysaccharides. *Biochimica et Biophysica Acta - General Subjects*, 1863(6), 1015–1026. <https://doi.org/10.1016/j.bbagen.2019.03.013>
- Tejado, A., Alam, M. N., Antal, M., Yang, H., & van de Ven, T. G. M. (2012). Energy requirements for the disintegration of cellulose fibers into cellulose nanofibers. *Cellulose*, 19(3), 831–842. <https://doi.org/10.1007/s10570-012-9694-4>
- Vlasenko, E., Schüle, M., Cherry, J., & Xu, F. (2010). Substrate specificity of family 5, 6, 7, 9, 12, and 45 endoglucanases. *Bioresource Technology*, 101, 2405–2411. <https://doi.org/10.1016/j.biortech.2009.11.057>
- Wang, J., Tavakoli, J., & Tang, Y. (2019). Bacterial cellulose production, properties and applications with different culture methods – A review. *Carbohydrate Polymers*, 219(May), 63–76. <https://doi.org/10.1016/j.carbpol.2019.05.008>
- Wei, J., Chen, Y., Liu, H., Du, C., Yu, H., Ru, J., ... Zhou, Z. (2016). Effect of surface charge content in the TEMPO-oxidized cellulose nanofibers on morphologies and properties of poly(N-isopropylacrylamide)-based composite hydrogels. *Industrial Crops and Products*, 92, 227–235. <https://doi.org/10.1016/j.indcrop.2016.08.006>
- Westereng, B., Arntzen, M. T., Aachmann, F. L., Várnai, A., Eijssink, V. G. H., & Agger, J. W. (2016). Simultaneous analysis of C1 and C4 oxidized oligosaccharides, the products of lytic polysaccharide monoxygenases acting on cellulose. *Journal of Chromatography A*, 1445, 46–54. <https://doi.org/10.1016/j.chroma.2016.03.064>
- Yang, X., Han, F., Xu, C., Jiang, S., Huang, L., Liu, L., ... Xia, Z. (2017). Effects of preparation methods on the morphology and properties of nanocellulose (NC) extracted from corn husk. *Industrial Crops and Products*, 109(July), 241–247. <https://doi.org/10.1016/j.indcrop.2017.08.032>
- Yue, Y., Wang, X., Han, J., Yu, L., Chen, J., Wu, Q., ... Jiang, J. (2019). Effects of nanocellulose on sodium alginate/polyacrylamide hydrogel: Mechanical properties and adsorption-desorption capacities. *Carbohydrate Polymers*, 206(October 2018), 289–301. <https://doi.org/10.1016/j.carbpol.2018.10.105>
- Zhang, K., Zhang, Y., Yan, D., Zhang, C., & Nie, S. (2018). Enzyme-assisted mechanical production of cellulose nanofibrils: Thermal stability. *Cellulose*, 25(9), 5049–5061. <https://doi.org/10.1007/s10570-018-1928-7>
- Zhao, Y., Moser, C., Lindström, M. E., Henriksson, G., & Li, J. (2017). Cellulose nanofibers from Softwood, Hardwood, and tunicate: Preparation-structure-Film performance interrelation. *ACS Applied Materials & Interfaces*, 9(15), 13508–13519. <https://doi.org/10.1021/acsami.7b01738>
- Zhou, H., St. John, F., & Zhu, J. Y. (2019). Xylanase pretreatment of wood fibers for producing cellulose nanofibrils: A comparison of different enzyme preparations. *Cellulose*, 26(1), 543–555. <https://doi.org/10.1007/s10570-019-02250-1>
- Zhu, H., Fang, Z., Preston, C., Li, Y., & Hu, L. (2014). Transparent paper: Fabrications, properties, and device applications. *Energy & Environmental Science*, 7, 269–287. <https://doi.org/10.1039/C3EE43024C>